Kovove Mater. 50 2012 177–184
DOI: 10.4149/km_2012_3_177

Nature of phases in boronized H11 hot work tool steel

P. Jurči[1]*, M. Hudáková[2], M. Kusý[2]

[1] *CTU in Prague, Faculty of Mechanical Engineering, Karlovo nám. 13, CZ-121 35 Prague, Czech Republic*
[2] *STU, MtF in Trnava, J. Bottu 52, SK-917 24 Trnava, Slovak Republic*

Received 17 December 2010, received in revised form 28 October 2011, accepted 7 November 2011

Abstract

The H11 hot work tool steel was short-time boronized, austenitized, quenched and tempered to a standard core hardness of 47–48 HRC. Microstructure, phase constitution and microhardness of boronized layers were investigated. It was found that the boronizing begins with the formation of α-solid solution, enriched with boron, and continues with the development of firstly the Fe_2B-boride compound and finally with the FeB-phase. During the boronizing, carbon atoms are transported from the surface towards the parent material. They are accumulated in a narrow intermediate region beneath the borides, where they develop new carbides. These carbides were identified as $M_{23}C_6$. Their portion probably increases with prolonged boronizing time, which is reflected in higher hardness of intermediate region. Also the hardness of boron compounds was found to be increased slightly with longer processing time.

K e y w o r d s: powder boronizing, H11 hot work tool steel, microstructure, phase constitution, borides, carbides

1. Introduction

Hot work tool steels are nowadays widely used in variety of industrial operations like lightweight alloys die casting, pressing, hot extrusion of metals, etc. In view of that, they have to withstand various degradation processes. Therefore, the materials must have an acceptable quality and the tools made from them have to be subjected to the heat treatment before use. A proper heat treatment gives them an appropriate hardness, toughness, wear resistance and other important properties.

Hot work tool steels contain typically of about 0.4 % C and 5 % Cr. Besides these main elements, they are alloyed also with small amounts of vanadium and molybdenum. In the soft-annealed state, the steels are composed by the ferrite and spheroidized carbides of $M_{23}C_6$ and/or M_7C_3-type. The quality of the hot work steels is prescribed in the NADCA 207--97 standard [1]. Accordingly, the carbides should be distributed uniformly throughout the matrix. Neither carbide clusters nor remaining as-cast networks are allowed. The standard heat treatment of tools made from hot work steels includes a step-like austenitizing, nitrogen gas quenching and triple tempering. After this procedure, the material should contain tempered martensite only, or with a negligible amount of undissolved carbides. Again, neither clusters nor carbide networks are acceptable for proper functionality of the tools. In addition, also the quenching has to be carried out in a right way, to avoid the precipitation of secondary carbides at the grain boundaries.

Boronizing belongs to the group of thermochemical processes used for the surface modification of metallic materials. As a product of the treatment, thin, very hard wear resistant and corrosion resistant compound layers are formed. Below the compound layers, transition areas are formed as a result of certain, but very limited solid solubility of boron in the α-(or γ)--phase. These areas, however, have significantly lower hardness than the boron compounds. Depending on the nature of the substrate material and processing conditions, single phase (Fe_2B) or double phase (FeB + Fe_2B) layers can be formed. If the material con-

*Corresponding author: tel./fax: +420 224357275; e-mail address: p.jurci@seznam.cz

tains a sufficiently high amount of chromium, also the chromium based or complex (Fe, Cr)-borides are formed [2, 3]. Carbon is almost completely insoluble in the borides. Therefore, it is moved into the substrate and forms a "carbide excess" in the transition areas, in high carbon steels in particular. The "carbide excess" is known from some investigations published previously [4], however, no relevant information on the nature of carbides was published yet. It should be noticed that the identification of the carbides is relatively difficult. They are highlighted only after subsequent heat treatment, when a part of original carbides is dissolved in the solid solution and insoluble part of carbides becomes easily visible. In addition, a very precise experimental technique is needed to obtain relevant experimental data.

Thickness of boronized compound layers is typically up to 0.4 mm. The thickest layers are formed on low carbon steels. Increasing carbon content leads to decrease of the layer thickness [4]. Also, according to Campos [5], chromium inhibits the layer growth. In the case of boronizing of high chromium steels, in addition, the FeB-layer tends to form more easily and, as indicated for instance by Dybkov et al. [3], Li et al. [6], and Oliveira et al. [7], it can make up to 50 % of the total compound layer thickness.

The adhesion of boron compound onto the steel substrate is commonly good because it is enhanced by the morphology of the interface between the substrate and the compound layer. The morphology of the interface depends on many factors. In low and medium carbon steels, the interface morphology is typically described as "sawtooth" [8]. Higher carbon content promotes alterations of the interface morphology. Kulka and Pertek [4], for instance, reported that in pre-carburized low carbon steels, the borides lost the "sawtooth" morphology and the interface became weak. Also for other high carbon cold work tool steels, similar phenomena were observed [9, 10]. For alloyed steels, Carbucichio and Palumbarini [11] established that the substitutional atoms like Mo, Cr and V concentrated at the tips of boride columns and reduced the boron flux in this region. As a result, the interface obtained an irregular form [7].

The Fe_2B single phase layer has normally a hardness between 1400 and 1700 HV and fracture toughness around 5–6 MPa $m^{1/2}$ [6, 9, 12, 13]. For the double-phase layer, the hardness is commonly higher because the hardness of FeB exceeds 2000 HV for carbon steels and often also 2200 HV for higher alloyed materials, for instance ledeburitic tool steels [2, 13]. The fracture toughness of the FeB-phase is two – four times lower than that of the Fe_2B-phase [12].

In the present paper we attempted to clarify the nature of phases formed in short-time powder boronizing of widely used H11 hot work tool steel.

2. Experimental

2.1. Material

The hot work steel of H11-type (THYROTHERM 2343 EFS) with 0.37 % C, 1 % Si, 5.3 % Cr, 1.3 % Mo, 0.3 % V, Fe bal. chemical composition (in wt.%) has been used for experimental investigations. Round shaped plate specimens of 20 mm in diameter and 5 mm in thickness were fine ground to a surface roughness of $R_a = 0.3$ μm.

2.2. Processing

The specimens were cleaned, degreased and boronized using the Durborid® powder mixture in hermetically sealed containers at a temperature of 1030 °C for 30, 45, 75 and 150 min. After the boronizing, the containers with specimens were furnace cooled down slowly to an ambient temperature, and then the specimens were removed. Subsequently, boronized samples were subjected to standard vacuum heat treatment. This procedure consisted of step-like heating up to the austenitizing temperature of 1020 °C, holding time for 30 min, nitrogen gas quenching (pressure of 6 bar) and triple tempering. Each tempering cycle took 2 h. The first tempering temperature was 570 °C, the second one 610 °C and the third one 550 °C. After each tempering cycle, the samples were cooled down slowly to a room temperature. Resulting core hardness of the steel was 47 HRC.

2.3. Characterization

Boronized specimens were metallographically prepared, e.g. ground and diamond suspension polished. For the light microscopy observations, the samples were standardly Nital etched for 10 s. For the examination using SEM, a deep Nital etching has been used. The light microscope Neophot 32 and field emission scanning electron microscope JEOL 7600 have been used. For the microstructural evaluation, an acceleration voltage of 15 kV has been used. But, it was lowered to 1 kV for the EDS mapping and point chemical analysis. For the EDS-analysis of boronized layers and carbides below, twenty measurements were made and the mean values and standard deviations were calculated.

Microhardness of boronized layers, transient regions and core material was measured with a Hanemann indenter placed in a Zeiss Neophot 32 light microscope, at a load of 100 g (HV 0.1). Ten measurements of microhardness were made in any of typical zones, e.g. FeB (if occurred), Fe_2B and intermediate region. The mean value, standard deviation and statistical analysis at a probability level of 95 % have been calculated from obtained sets of results [15].

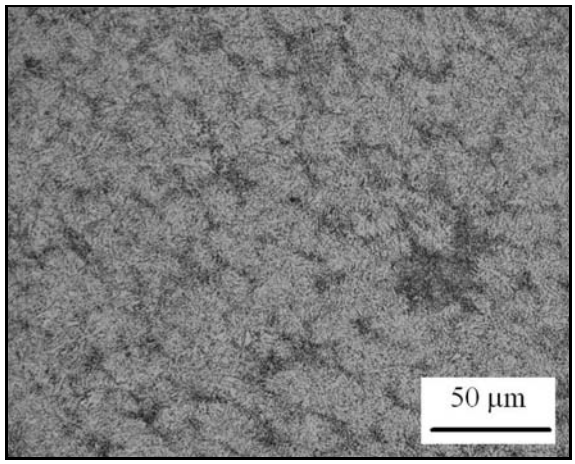

Fig. 1. Light micrograph of the microstructure of as-received H11 steel.

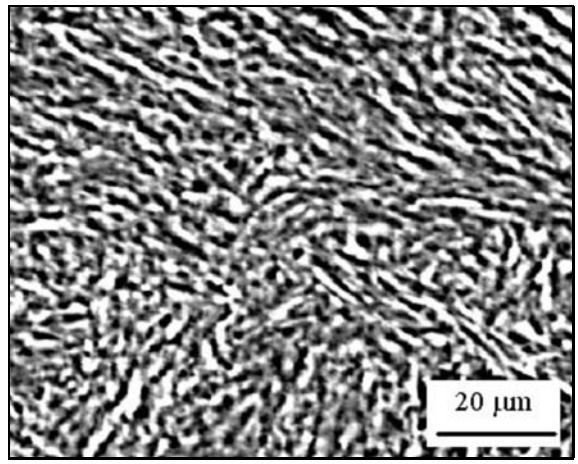

Fig. 2. Showing the microstructure of the bulk material after heat treatment.

X-ray patterns of as-delivered material and the boride layers were recorded using a Phillips PW 1710 device with Fe filtered $Co_{\alpha 1,2}$ characteristic radiation. Detector arm was equipped with monochromator. Data were recorded in the range from 20–144° of the two-theta angle with step 0.05° and counting time per step 5 s. Firstly, boronized layers have been examined as prepared. Subsequently, 20 μm of surface layer was removed by classical metallographical fine grinding and the measurement has been repeated. After that, again 20 μm of surface volume was removed. This approach has been repeated until the whole boron compound was removed. Note that the data recorded from each X-ray pattern do not represent only the surface phase constitution but, with respect to the penetration depth of X-rays, also the phase constitution of a certain material volume. Therefore, the data recorded at any depth below the surface represent the phase constitution of the material in thin layer below the grinding depth indicated in the diagrams.

The identification of peaks was made by comparison of calculated interplanar spacings with the d_{hkl} list of relevant phases taken into consideration from as the material composition so expected phases according the Fe-B and Fe-Cr-B phase diagrams. All the crystallographic data were taken from the Pearson's handbook [14].

3. Results, discussion

Microstructure of the as-received material consisted of ferritic matrix and uniformly distributed spheroidized carbides, Fig. 1. Neither carbide clusters nor remaining as-solidified carbide networks were found. It indicates that the material used for the investigations was of an acceptable quality.

Microstructure of the bulk material after standard heat treatment, Fig. 2, consisted of fine tempered martensite. The material contained only martensitic needles, uniformly distributed throughout the specimen. Neither presence of undissolved carbides nor proeutectoidal phases at the grain boundaries has been established. These facts confirm that the heat treatment after the boronizing was performed in an appropriate way.

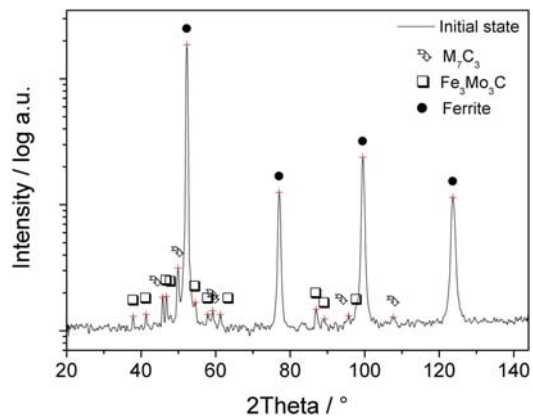

Fig. 3. X-ray patterns of the as-received material.

X-ray diffraction, Fig. 3, fixed the α-phase as the major constituent of the as-received steel. The minor phases are the carbides, namely chromium rich M_7C_3--carbide and also combined Fe/Mo carbide M_6C.

Boronized layers formed at 1030 ℃ for 30 and 45 min consisted only of the Fe_2B-phase, Fig. 4a,b. The compound layer developed at the same temperature but for the processing time of 75 min exhibited symptoms of presence of the FeB-phase in the close vicinity of the surface, Fig. 4c. The presence of the FeB-phase is evident, due to the occurrence of parallel cracks with the surface. The cracking of two-phased boronized layers is immanent for them since the phases FeB

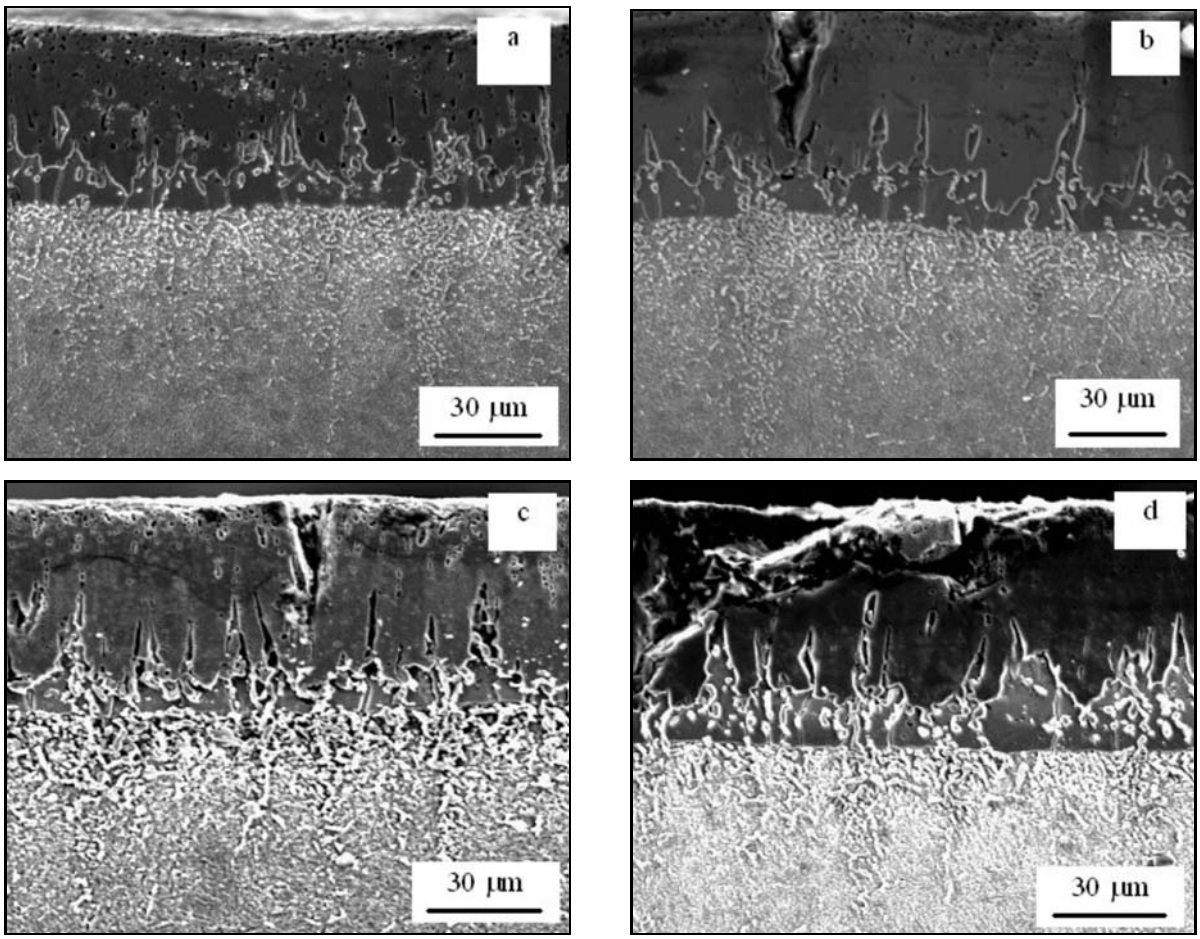

Fig. 4. Showing boronized layers on the H11-steel surface formed at 1030 °C for: a) 30 min, b) 45 min, c) 75 min, d) 150 min.

and Fe_2B contain high, and opposite oriented stresses, which together with their brittleness makes it easily to crack. Also the region formed for 150 min exhibits two phases, Fig. 4d. But, the FeB-region was much thicker than that formed for 75 min.

Below the boronized compound layers there were the intermediate regions. These regions are typical by elevated portion of undissolved carbides. The density of carbides was maximal at the compound layer interface and it decreased towards the substrate. The cause of formation of these carbides can be explained simply by the fact that carbon is not soluble in the borides. During the boronizing, the flux of carbon atoms is oriented towards the core material. Carbon atoms are accumulated in narrow intermediate region, close below the boron compound and due to their high affinity to the atoms of iron and alloying elements, carbides are formed. Subsequent austenitizing was carried out to a temperature leading to complete dissolution of the original carbides. This was confirmed also in our present work, Fig. 2. But, the newly developed carbides ("carbide excess") in the transient areas correspond to a "new equilibrium", and they underwent the dissolution in the austenite only in a limited extent.

Detail SEM micrograph from the intermediate region from the sample boronized at 1030 °C for 75 min is in Fig. 5a. On the right side of the micrograph, there is the compound layer. Remaining part of the micrograph shows the intermediate region. As shown, the matrix of the material is formed by tempered martensite. The carbides have different size and shape. Larger particles with sharp edges have a length of around 5–7 μm and a width of few microns. Finer, spherical carbides have a diameter generally below 1 μm. EDS--maps made from the region in Fig. 5a indicate that the carbides contain enhanced portion of chromium, Fig. 5b, but reduced amount of silicon, Fig. 5c and slightly also iron, Fig. 5d.

These results confirm the abovementioned consideration on limited solubility of the "new" carbides in the austenite. From the size and shape of the carbides one can assume that while the larger particles remained stable during austenitizing the smaller spherical carbides underwent the dissolution.

It is not surprising that the carbides contain more

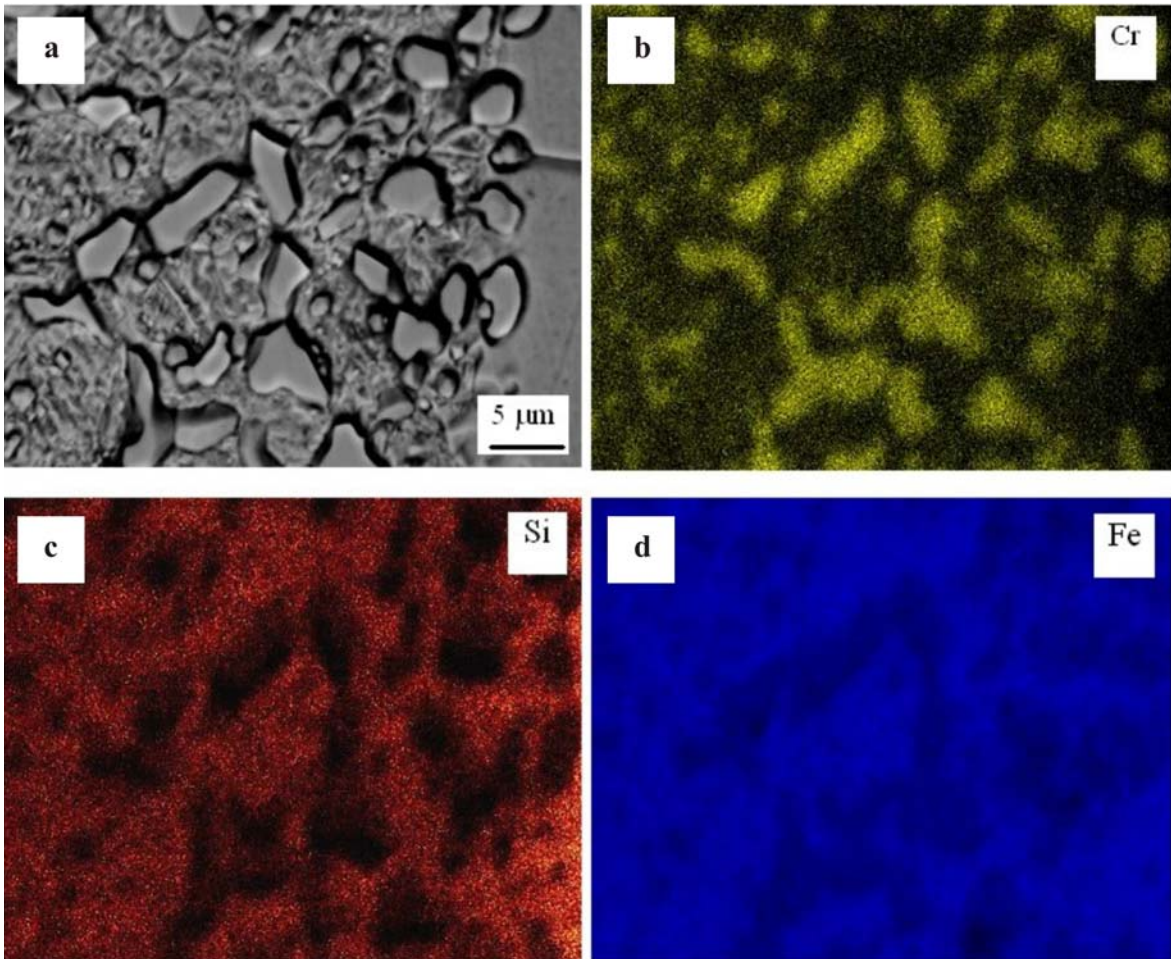

Fig. 5a–d. Showing the intermediate region of boronized layer formed at 1030 °C for 75 min and corresponding EDS-maps.

chromium than the matrix after the heat processing. The original phase of the material is, besides the alpha-phase, the M_7C_3-carbide. The M_7C_3-carbide comprises the chromium, but it can contain also iron (up to a ratio Cr : Fe of around 1 : 1) and small portion of other elements if the alloy contains them in a sufficiently high amount. Due to complete dissolution of the M_7C_3-carbides during the boronizing, the matrix contained a high portion of Cr. This is why chromium formed the carbides in the intermediate region. Besides Cr, the carbides contained also iron, but in slightly lower amount than the matrix, Fig. 5d. On the other hand, silicon did not enter into the carbides and it is dissolved in the matrix, Fig. 5c.

X-ray diffraction made from the surface confirmed that the compound layer on the specimen processed at 1030 °C for 30 min is formed only of the Fe_2B-boride, Fig. 6a. The measurements of (020) interplanar spacings indicated slight disagreement with the interplanar spacing of the pure Fe_2B. The (020) – diffraction peak was shifted to lower value of the two-theta angle that is typical for the cases when the elements with bigger atomic radii enter into the compound. In our case it is especially the chromium that can be expected to be dissolved in the Fe_2B. The atomic radius of Cr is 0.1423 nm and that of Fe is 0.1411 nm [16]. Therefore, the shifting of the (020) – diffraction line to lower diffraction angle can be considered as logical. It should be noted that similar shifting of the (020) – diffraction line of Fe_2B-phase has been recorded for the layers formed at other combinations of processing parameters, also.

The total thickness of compound layer was estimated to be of about 80 μm. This is why also in a depth of 80 μm below the surface, tracks of Fe_2B-phase were found. However, also the diffraction peaks from the α-phase were identified due to the penetration of X-rays into a certain depth below surface after a removal of 80 μm of the material, Fig. 6b. After a removal of 160 μm, no borides were identified, Fig. 6c. On the other hand, besides the major constituent α-phase, peaks from the $M_{23}C_6$-carbide were fixed.

Obtained results show that the carbides in the intermediate region are of the $M_{23}C_6$-type. In the carbon-chromium equilibrium diagram, there is the pure $Cr_{23}C_6$-phase at a carbon content of 5.5–5.8 wt.%

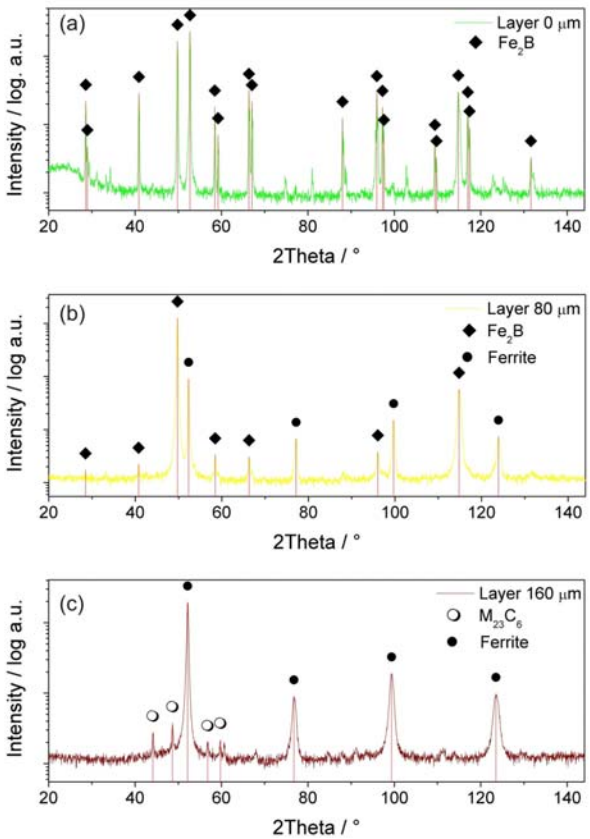

Fig. 6. Showing X-ray patterns of boronized layer made at 1030 ℃ for 30 min: a) surface, b) 80 μm below the surface, c) 160 μm below the surface.

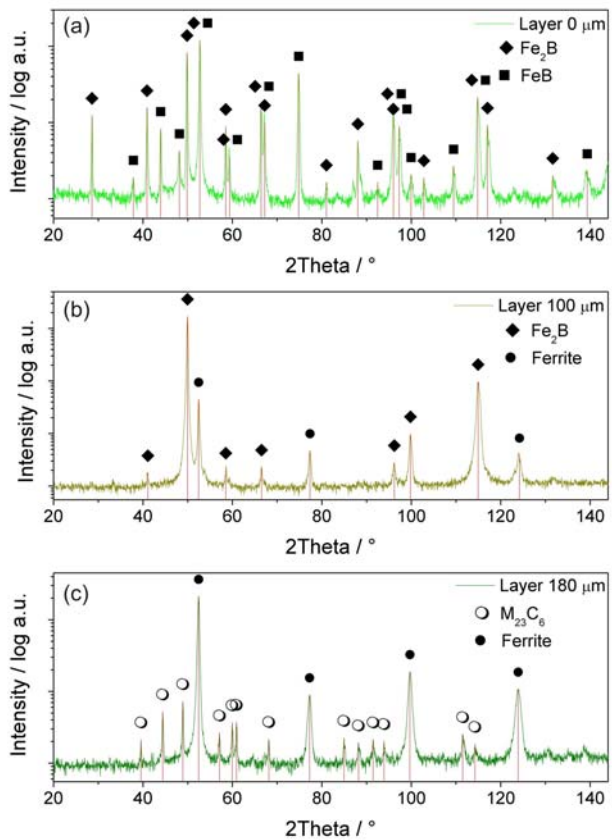

Fig. 7. Showing X-ray patterns of boronized layer made at 1030 ℃ for 75 min: a) surface, b) 100 μm below the surface, c) 180 μm below the surface.

and the pure Cr_7C_3-phase at a carbon content of 9 wt.%, respectively. Other possible carbide, which could have been expected to be formed, is the cementite. However, due to dissolution of original M_7C_3--carbides in the austenite, the matrix contains a high amount of chromium. Therefore, the formation of the cementite is not probable. From two abovementioned chromium-based phases, the $M_{23}C_6$-phase contains less carbon than the M_7C_3. It is thus logical that the $M_{23}C_6$-carbides have been firstly formed below the compound borides during the boronizing. The M_7C_3--carbides were not found in boronized and subsequently heat processed material. However, this phase is the equilibrium one for a given system, Fig. 3. Therefore, one would expect also its formation due to the carbon atom transport out from the boronized compound layers. It seems only that the processing time is not long enough to promote sufficient carbon redistribution in the near surface region of the material, required for the M_7C_3-carbide development.

The boronized layer formed for the processing time of 45 min behaved in a very similar manner than that made for 30 min. Neither the differences in phase constitution of the compound borides nor of the intermediate region were found from the qualitative point of view.

Boron compound layers formed on the samples processed for 75 min differ from those developed for shorter processing times in the occurrence of FeB--peaks, Fig. 7a. This corresponds well with the metallographical observations, Fig. 4c, where clear symptoms of the presence of thin FeB-phase sub-layer were found. Greater thickness of the boronized layers was reflected only in the thickness of each sub-layer, with no presence of other phases or structural constituents, Figs. 7a–c.

Figure 8 shows the X-ray patterns from the boronized material processed at 1030 ℃ for 150 min. The surface-face region is formed primarily by the FeB--phase, Fig. 8a. Lower part of the compound boron layer contained mainly the Fe_2B-phase, Fig. 8b. These observations correspond very well with the metallography, Fig. 4d, where it is evident that the FeB takes off approximately 30 % of the total boron layer thickness. Moreover, it is also evident that the Fe_2B--sub-layer had not uniform thickness since the interface between compound layer and parent material clearly exhibited "sawtooth" morphology. This is

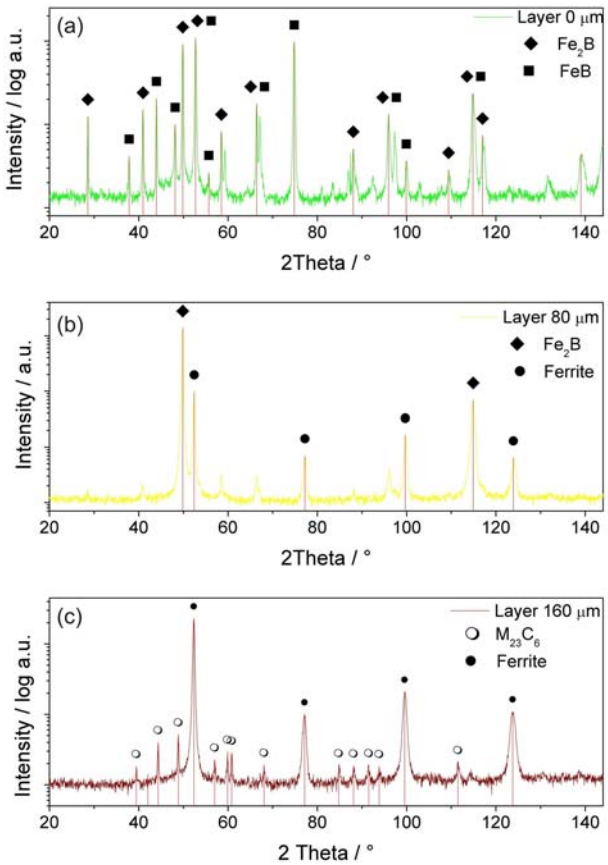

Fig. 8. Showing X-ray patterns of boronized layer made at 1030 ℃ for 150 min: a) surface, b) 80 μm below the surface, c) 160 μm below the surface.

also a principal explanation why the X-ray diffraction from the depth of 80 μm fixed also the α-phase besides the Fe_2B. X-ray diffraction made in the depth of 160 μm below the surface fixed also $M_{23}C_6$-carbide besides the α-phase. It indicates that there is not difference in the nature of carbides formed in intermediate region due to "carbon excess" in the samples processed for various processing times. The statement above on the carbon atoms flux during the boronizing, needed for the formation of stable M_7C_3-phase, is valid also for the processing time of 150 min.

Hardness measurements of boronized layers are summarized in Table 1. If the development of boron rich phases is finished with the Fe_2B-compound formation, then its hardness ranged close below 1500 HV 0.1, while the hardness of the layers formed for different (but short) processing time does not differ. Intermediate regions enriched with carbides had the hardness between 406 and 416 HV 0.1 and they also did not differ from the statistical point of view, with a probability of 95 %.

Boronized layers formed for 75 and 150 min, respectively, are two-phased. The FeB had a hardness exceeding 2200 HV 0.1, Table 1. It is in good agreement with the early observations by Hudáková et al. [2] and Campos et al. [13] made on other high alloyed steels. The Fe_2B-sub-layers exhibited also higher hardness than those developed for shorter processing times. The mean values were 1792 and 1686 HV 0.1, respectively, with relatively large dispersion of results. In this case, higher hardness can be attributed to formation of not only iron containing borides, but also borides of alloying elements, mainly chromium. Finally, also the intermediate regions had increased hardness compared to those formed for the processing times 30 and 45 min, respectively. The nature of this phenomenon is not entirely clear yet. The image analysis of carbide portion, which might confirm this fact, was not a goal of this study. Nevertheless, one can assume that increased hardness is due to enhanced portion of carbides in these regions. From the Fig. 4 it seems that the assumption looks to be natural. Also other consideration supports that – as the boronized layer becomes thicker and thicker, more carbon atoms are transported into the core material and more carbides can be developed. Since the $M_{23}C_6$-phase has a hardness ranging between 1000 and 1200 HV [17], which is two-three times higher than the matrix, increased hardness with an increased portion of $M_{23}C_6$ carbides is logical to be expected.

4. Conclusions

Obtained experimental results show that:

1. As-received steel contains the alpha-phase and

Table 1. Hardness of typical regions of boronized layers

Boronizing	Microhardness HV 0.1		
	FeB	Fe_2B	intermediate region
1030 ℃/30 min	Not detected	1483 ± 89	416 ± 20
1030 ℃/45 min	Not detected	1473 ± 88	406 ± 62
1030 ℃/75 min	2221 ± 118	1792 ± 192	638 ± 41
1030 ℃/150 min	2345 ± 251	1686 ± 111	589 ± 38

M_6C and M_7C_3-carbides. After the heat treatment the microstructure of the steel is fully martensitic, without any symptoms of presence of undissolved carbides.

2. The boronizing of H11 hot work tool steel begins with the formation of alpha solid solution, containing boron. After the boron solubility in alpha phase is exceeded, Fe_2B and afterwards FeB-phases are formed.

3. The Fe_2B-phase was enriched with alloying elements, with the chromium in particular. This was detected by the shifting of two-theta diffraction lines to lower value compared to those of pure Fe_2B.

4. During the boronizing, carbon diffuses towards the substrate and is accumulated in narrow intermediate region. New carbides are formed in this region, due to new equilibrium determined by enhanced carbon content here.

5. These carbides are the $M_{23}C_6$. It seems that, with prolonged boronizing time, their portion increases due to more intensive carbon transport out from the boronized substrate, which is reflected in elevated hardness of intermediate regions formed for longer processing times.

6. Also, the hardness of compound layers slightly increases with longer processing time, which can be attributed to increasing saturation of the surface region with boron.

References

[1] NADCA 207-97 Recommended Procedures for H-13 Tool Steel, North American Die Casting Association 1997.

[2] Hudáková, M., Kusý, M., Sedlická, V., Grgač, P.: Materials and Technology, *41*, 2007, p. 81.

[3] Dybkov, V. I., Lengauer, W., Barmak, K.: J. Alloys Compd., *398*, 2005, p. 113. doi:10.1016/j.jallcom.2005.02.033

[4] Kulka, M., Pertek, A.: Appl. Surf. Sci., *218*, 2003, p. 161. doi:10.1016/S0169-4332(03)00303-9

[5] Campos, I., Torres, R., Ramirez, G., Ganem, R., Martinez, J.: Appl. Surf. Sci., *252*, 2006, p. 8662. doi:10.1016/j.apsusc.2005.12.002

[6] Li, Ch., Shen, B., Li, G., Yang, Ch.: Surf. Coat. Techn., *202*, 2008, p. 5882.

[7] Oliveira, C. K. N., Casteletti, L. C., Lombardi Neto, A., Totten, G. E., Heck, S. C.: Vacuum, *84*, 2010, p. 792. doi:10.1016/j.vacuum.2009.10.038

[8] Uslu, I., Omert, H., Ipek, M., Celebi, F. G., Ozdemir, O., Bindal, C.: Materials and Design, *28*, 2007, p. 1819. doi:10.1016/j.matdes.2006.04.019

[9] Ozbek, I., Bindal, C.: Surf. Coat. Techn., *154*, 2002, p. 14. doi:10.1016/S0257-8972(01)01409-8

[10] Sen, S., Ozbek, I., Sen, U., Bindal, C.: Surf. Coat. Techn., *135*, 2001, p. 173. doi:10.1016/S0257-8972(00)01064-1

[11] Martini, C., Palombarini, G., Poli, G., Prandstraller, D.: Wear, *256*, 2004, p. 608. doi:10.1016/j.wear.2003.10.003

[12] Sen, U., Sen, S.: Mater. Charact., *50*, 2003, p. 261. doi:10.1016/S1044-5803(03)00104-9

[13] Campos, I., Farah, M., Lopez, N., Bermudez, G., Rodriguez, G., Villa Velazquez, C.: Appl. Surf. Sci., *254*, 2008, p. 2967. doi:10.1016/j.apsusc.2007.10.038

[14] Villar, P., Calvert, L. D.: Pearson's Handbook of Crystallographic Data for Intermetallic Phases. Vol. 1. Metals Park, Ohio, American Society for Metals 1989.

[15] Kučerová, M.: Application of method of planned experiments in the quality management. Trnava, Alumni Press 2010.

[16] Cahn, R. W.: Physical Metallurgy, 2nd revised edition. Amsterdam – London, North-Holland Publishing Company 1970.

[17] Geller, J. A.: Tool Steels (Instrumentalnyje stali), 5th issue. Moscow, Metallurgija 1983.